EVALUATION OF THE MICRO WOBBLE MOTOR FABRICATED BY CONCENTRIC BUILD-UP PROCESS

K.Nakamura, H.Ogura, S.Maeda, U.Sangawa, S.Aoki and T.Sato
Matsushita Research Institute Tokyo, Inc.
3-10-1 Higashimita, Tama-ku, Kawasaki-shi, Kanagawa 214, Japan

ABSTRACT

We proposed a CB (concentric build-up) process to fabricate the electrostatic wobble motors in MEMS '94[1]. This process features the concentric build-up of layers around a cylindrical substrate and produces three dimensional bulk structures using newly developed microfabrication technique. This time, we have successfully measured the wobbling motion and estimated key motor parameters such as rotation rate, rotor-stator gap, output torque and surface condition of stator and rotor. This method facilitated the evaluation of the motors and processes. And we have located the causes of torque deterioration.

1 INTRODUCTION

The rotation characteristics of the wobble motor is dominated by the accuracy in forming the rotor-stator gap. And its dynamic motion, for example slew range or pullout torque, is limited by friction at bearing mechanism and slip at the rotor-stator contact. In these days micro motor research is beginning to focus on these basic phenomena.

In order to measure the friction, a special technique is proposed[2], where the rotor is picked out from the motor and tested under the equipment especially developed. But it is more simple and convenient to estimate the friction from the relation between the applied voltage and the rotor rotation in situ experimentally in operation[3][4]. The latter method requires the assumption that the calculated electro-static force is actually acting on the rotor. These micro wobble motors were fabricated by planar machining technique, so the rotor thickness are within 100 μm. This thickness cannot produce the high output torque, but the uniformity of rotor-stator gap in this thickness may satisfy this assumption.

As the wobble motor fabricated by CB process has rotor-stator gap of less than 20 μm, 5 mm of stator length and 3.5 mm in stator electrode length(Figure 1), it is important to keep the longitudinal rotor-stator gap accurate for producing the ideal large torque and designed rotation rate. In order to analyze this narrow and long gap under the condition where the rotor and stator are in a unit, we tried to measure the wobbling motion directly, which will reveal the gap condition.

In this paper we present the method to measure the wobbling dynamics, and estimate this important gap. The dynamic torque is also obtainable.

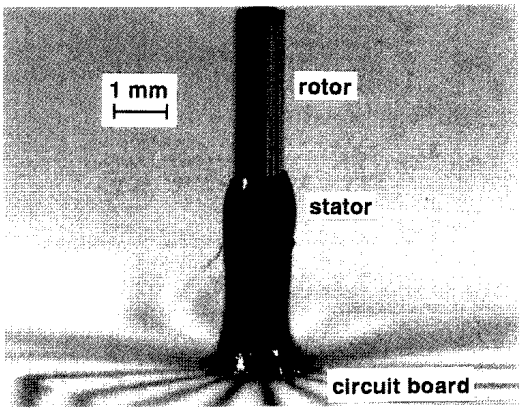

Figure 1. The whole view of the fabricated wobble motor

2 MOTOR DESIGN AND FABRICATION

Figure 2 shows the CB process for the wobble motor. The fabrication procedure is reviewed in the following.

1)The ZrO_2 cylindrical substrate with 1 mm diameter, 1 μm roundness and 0.02 μm Ra surface roughness, is prepared as a rotor shaft. Then the metal film of Ti and Pt are deposited in RF magnetron sputtering.

2)The $SrTiO_3$ insulate layer of 3.9 μm is deposited in RF magnetron sputtering. This thin film has specific dielectric constant of >100 at 1 kHz.

3)The sacrificial layer of 19.7 μm thickness is formed by dip-coating technique. We adopted polyimide because of its high etching rate.

4)The 16 pole stator electrodes with 3.5 mm length patterned by contact exposure technique, are formed using electroless plating and lift-off technique.

5)Au wires are bonded to the electrodes to connect the motor to its driving circuit. After bonding, resin is molded and stator is formed.

6)Finally, the sacrificial layer is dissolved selectively by butyloractone-solvent, and the rotor with insulator and the stator with electrodes are separated.

0-7803-2503-6 © 1995 IEEE

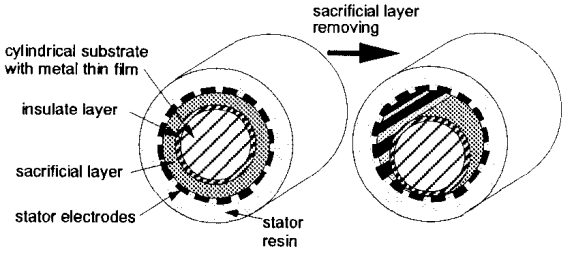

Figure 2. A cross section of the wobble motor fabricated by CB process

The specifications of the wobble motor we evaluated are summarized in Table 1. The expected gear ratio is calculated to be 25.6 from the rotor radius and rotor-stator gap which is equal to the sacrificial layer thickness.

Table 1. Specifications of the wobble motor

rotor	outer radius	504.5 μm (including metal and insulate layer)
	length	15mm
	material	ZrO_2
	mass	76 mg
	moment of inertia	9.9×10^{-12} kg·m^2
insulator	thickness	3.9 μm
	specific dielectric constant	100
sacrificial layer	thickness	19.7 μm
stator	inner radius	524.2 μm
	electrode length	3.5 mm
	number of poles	16
gear ratio	25.6	

Figure 3 shows the theoretical electro-static torque calculated by conformal mapping approximation[5]. The horizontal axis ξ is angular position of the voltage applied electrode relative to the rotor-stator contact. The voltage 250V is applied on a stator electrode and the others and the rotor are grounded.

When the rotor moves from one stator electrode to another, first, the starting torque is 1.7×10^{-5} N·m (ξ=-22.5°), second, the maximum torque (3.2×10^{-4} N·m) appears at ξ=-9°, and finally the motor stabilizes itself at ξ=0°.

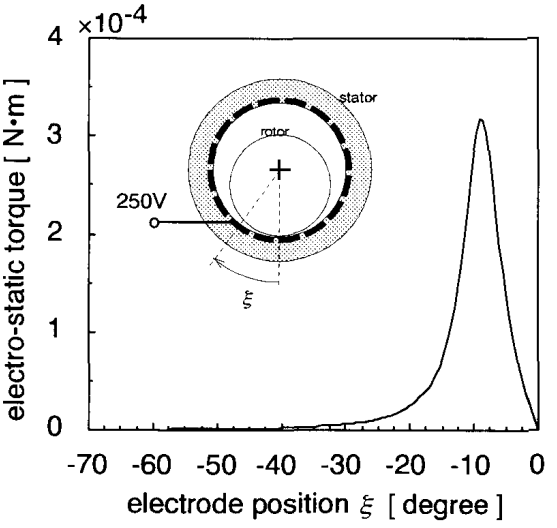

Figure 3. Calculated electro-static torque versus electrode position

3 THE WOBBLING MEASUREMENT SET-UP

As shown in Figure 4, a thin aluminum for rotation measurement is mounted on the top side of the rotor and a small pivot which has 35 μm tip radius is attached to the bottom side. The rotation rate is measured from the fiber photoelectric sensor which generates 1 pulse per rotation. The wobbling dynamic movement is measured in x and y direction by laser triangulation sensors.

Next, the motor is driven in the air atmosphere. The rotor is usually supported by flat glass plate, but the rotation without the pivot bearing can be easily achieved by placing the motor horizontally.

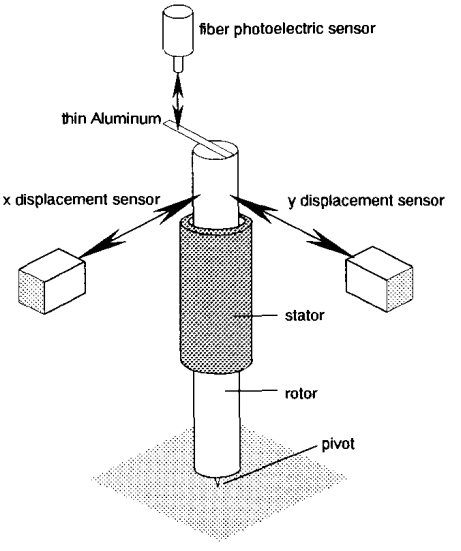

Figure 4. The wobble motor and laser sensors set-up

4 EXPERIMENT AND RESULT

As the first step, we measured the rotation rate in order to find the stable rotation conditions. In Figure 5, the relationship between driving pulse frequency and rotation rate are plotted with different stator voltages from 100V to 250V. The rotation rate is approximately in proportion to the low pulse frequency. In higher frequency, the motor loses synchronous rotation, and the rotation rate declines. The higher the applied voltage is, the more widely the proportional relationship is maintained. This result clearly shows that the higher driving voltage realizes more stable rotation. The straight solid line in figure 5 shows the theoretical values derived from the design parameters. The experimental rotation rate is less than 75% of the theoretical one. We attributed this difference to the narrowed rotor-stator gap.

In order to measure the real gap, we tried an experiment in which the rotor is rotated against the stator quasi-statically so that there is no slip between them. In the experiment the motor is held horizontally and the stator is turned slowly. Just then the rotor rotates itself by the gravity force. Figure 6 shows the rotor rotation times versus stator rotation times. From the experiment, the actual gear ratio is found to be 33.9 by line fitting. From this value, the actual gap separation can be calculated as 14.9 μm, which is 5 μm smaller than the design value of sacrificial layer. The straight dashed line in Figure 5 shows revised theoretical values using the gear ratio derived from the above experiment. This time, the experimental values coincide with theoretical ones.

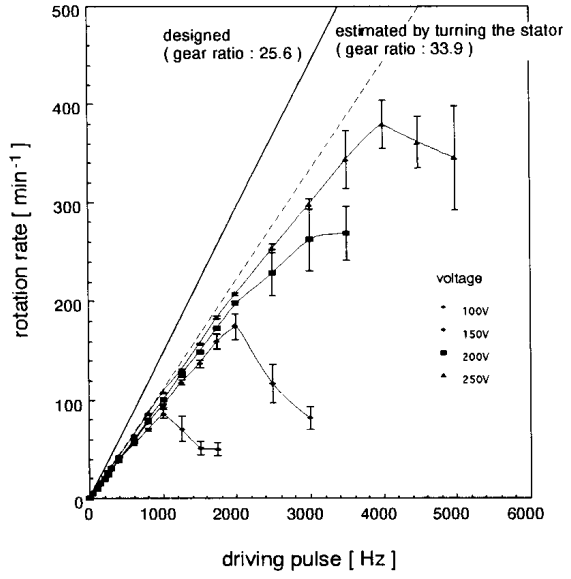

Figure 5. The measured rotation rate versus driving pulse frequency

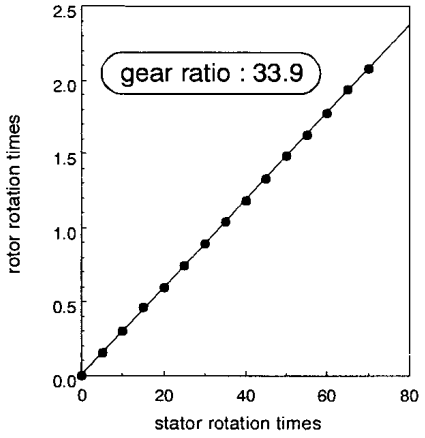

Figure 6. The measured gear ratio by turning the stator slowly

From this result, we adopted the standard driving condition of 250V at 200 Hz for the wobbling dynamics measurement. We presumed that the rotor rotates synchronously with driving pulse frequency and causes no slip at this condition.

Next, we measured the wobbling motion on the condition described above. In Figure 7 the measured positions of the center of the rotor are dotted and its ideal locus from the design is shown as a reference. Although the experimental results again don't match the ideal one, the wobbling radius of approximately 15 μm just coincide with the previous gap measurement result. This means that this technique correctly measure the gap separation. Moreover, as the trajectory in Figure 7 can be measured with high repeatability, we presume that it shows the surface condition of rotor and stator. The surface roughness predicted from the profile is approximately 1 μm.

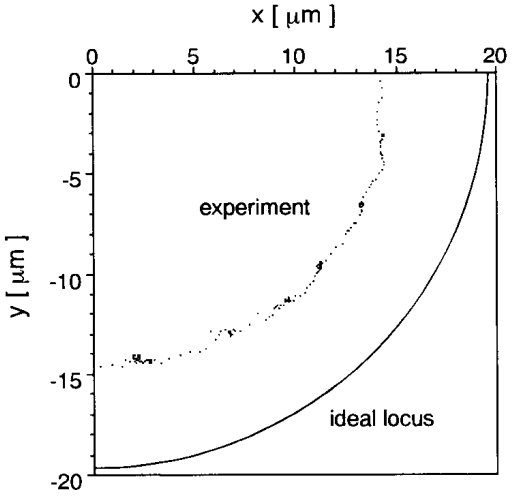

Figure 7. Trajectory of the center of rotor

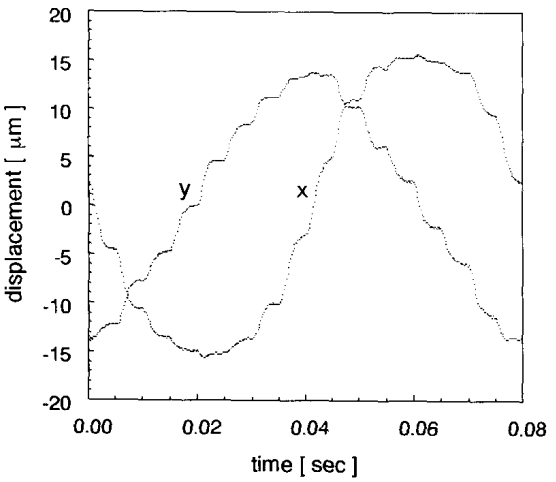

Figure 8. The measured wobbling motion in x and y directions during one period

Figure 8 shows the wobbling motion of x and y directions in time domain. At 200 Hz of this low driving frequency, the rotor behaves like step responses. From this data, angular acceleration of rotor can be calculated by numerical differentiation. The dynamic torque is calculated as a product of the angular acceleration, moment of inertia and reciprocal of gear ratio. The maximum dynamic torque was obtained in two conditions, with pivot bearing and without it. The results are shown in Table 2.

Table 2. The measured dynamic torque

	without pivot	with pivot
maximum dynamic torque	1.3×10^{-7} N·m	1.0×10^{-7} N·m

We cannot find the significant difference between the two experimental values. However they show a big deterioration compared with the theoretical static torque calculated in Figure 3.

In order to confirm the reliability of this value, we measured the maximum static torque by directly loading weights around the rotor. In figure 9 this method is shown where the rotor slightly pulled up the weight and keep it at a constant height. The maximum static torque was measured to be 2.0×10^{-7} N·m. This result coincide with the values obtained from the wobbling measurement in Table 2 in magnitude, validating the torque estimation from the wobbling motion.

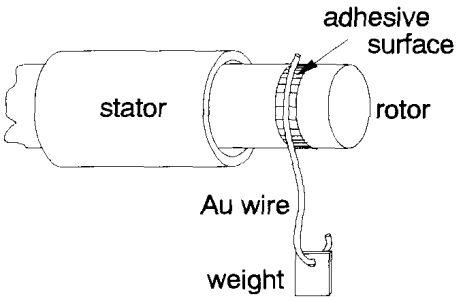

Figure 9. The static torque measurement method

5 DISCUSSION

The measured wobbling motion in Figure 7 clearly indicates that the real inner radius of the stator is 5 μm less than the design value and its inner profile has roughness about 1 μm. Hereafter we discuss the relation between this contracted and bumpy profile and the measured torque reduction

In order to examine the influence of these deformations, a simple model where the rotor-stator contact is obstructed by some defect with height h, is assumed and the electro-static torque is calculated again by conformal mapping method. In figure 10 the relationship between the electrode position ξ and the electro-static torque at 250V, are plotted with the height of defect of 0, 1, 3 and 5 μm respectively. The torque drop is sensitive to the height h. The surface roughness about 1 μm found in wobbling trajectory in Figure 7 may cause the torque reduction within the extent of 1/10. Moreover, supposing the rotor is kept 5 μm away from the stator electrode, the torque is reduced to less than 1×10^{-6} N·m. This situation can be possible when the stator contracts 5 μm, not uniformly but locally along the longitudinal direction of the stator.

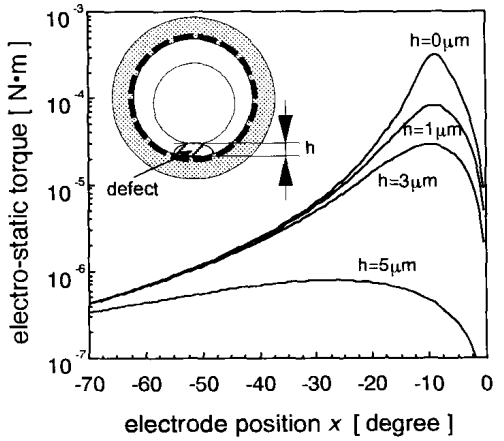

Figure 10. Calculated electro-static torque when the rotor-stator contact is obstructed by defects

In order to directly observe the surface condition of the stator, the stator was cut and observed by SEM. Figure 11 shows the inner surface of the stator just after the sacrificial layer was removed. The electrodes and stator resin have roughness about 0.07 μm Ra and 0.09 μm Ra respectively. Figure 12 is the surface after the motor was operated for several hours, indicating the damaged surface. Using the electron-beam 3D analysis, we carefully examined the surface roughness and found three types of defects.

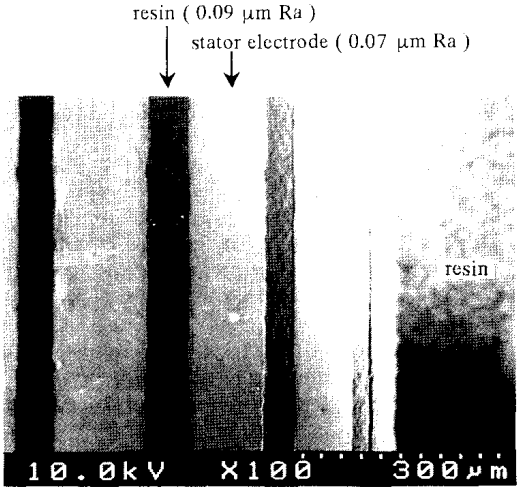

Figure 11. A SEM photograph of the inside of the stator after the sacrificial layer removal

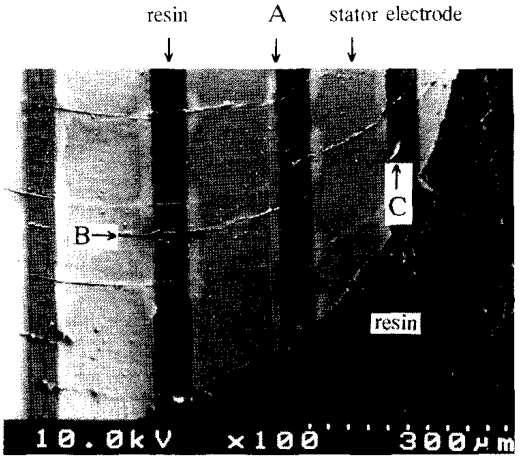

Figure 12. A SEM photograph of the inside of the stator after the motor operation

Defect A in Figure 12, which runs along the boundary between stator electrodes and stator resin, is resin burr of 0.5 μm high. We attribute the defect to lift-off process in which stator electrodes are patterned by removing underlying patterned resist.

Figure 13 is the sectional view of the motor after the electrodes are separated by lift-off process. The edge of the thin electrode is overhanging slightly from the sacrificial polyimide layer. The defect occurs at the spots where the stator resin is not filled enough along this edge.

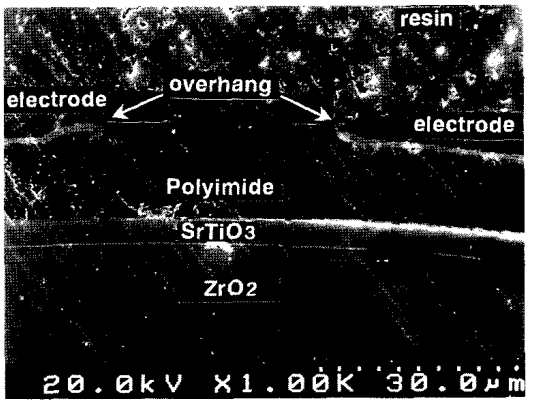

Figure 13. The sectional view of the motor which shows the over hanging of the electrode edge

Defect B, which runs across the stator and resin, is about 0.5 μm high. This type of defect is not observed before the operation in Figure 11. We presume it to be the scratches by dust particles after the motor operation, or to be caused by the released residual stress in the stator resin.

The other small pieces of about 1~2 μm, which seemed to be peeled off from the inside of the stator, are found (for example, C). This type also is not found in Figure 11, suggesting that the endurance of stator forming components is more required against the wobbling movement.

The size of these undesirable defects, 0.5 μm ~ 2.0 μm, coincides with the predicted roughness value from the rotor trajectory in Figure 7.

In the SEM observation, we couldn't find the steep contraction of 5 μm. We presume that this size of narrowed gap was due to the release of the residual stress in the stator resin. This phenomena may be related with the non-uniform thickness of the molded stator resin, which tends to cause much contraction around the thickest cross section.

6 CONCLUSION

In conclusion, we have developed wobbling motion measurement method which is useful in determining the rotor-stator gap, the torque and the surface condition of the stator. These results well coincided with the results by the other methods, rotating the stator quasi-statically, loading the weight and observing the surface by SEM respectively.

The experimental results suggested the problems which remained in CB process, for example the residual stress of the stator resin and the surface roughness of the stator. By the computer simulations we have confirmed that these discrepancies from the ideal stator cause the output torque deterioration.

We believe that this method will facilitate the motor evaluation and lead to the improvement of the CB process. We are also planning to expand the method so that it can tell the rotor-stator slip on the spot. This will pave the way to the evaluation of friction in a micromotor.

ACKNOWLEDGMENTS

This work was performed under the management of the Micro Machine Center as a part of the R&D of the Micromachine Technology supported by NEDO(New Energy and Industrial Technology Development Organization).

REFERENCES

[1] H.Ogura, *et al.*, "A Concentric Build-up Process to Fabricate Practical Wobble Motors," *Proc. IEEE MEMS*, 1994, pp.114-118.

[2] U. Wallrabe, *et al.*, "Friction measurements on LIGA-processed microstructures," *Journal of Micromechanics and Microengineering*, 1994, vol. 4-1, pp.14-22.

[3] V.R. Dhuler, *et al.*, "A Comparative Study of Bearing Design and Operational Environments for Harmonic Side-Drive Micromotors," *Proc. IEEE MEMS*, 1992, pp.171-176.

[4] U. Wallrabe, *et al.*, "Design rules and test of electrostatic micromotors made by the LIGA process," *Journal of Micromechanics and Microengineering*, 1994, vol. 4-1, pp.40-45.

[5] R. Mahadevan, "Analytical Modelling of Electrostatic Structures," *Proc. IEEE MEMS*, pp.120-127, 1990.